



An oleuropein rich-olive (*Olea europaea* L.) leaf extract reduces β -amyloid and tau proteotoxicity through regulation of oxidative- and heat shock-stress responses in *Caenorhabditis elegans*

Jose M. Romero-Márquez^{a,1}, María D. Navarro-Hortal^{a,1}, Victoria Jiménez-Trigo^a, Laura Vera-Ramírez^{a,b}, Tamara J. Forbes-Hernández^a, Adelaida Esteban-Muñoz^c, Francesca Giampieri^{d,e,f}, Pedro Bullón^g, Maurizio Battino^{d,h}, Cristina Sánchez-González^{a,i,**}, José L. Quiles^{a,f,*}

^a Department of Physiology, Institute of Nutrition and Food Technology “José Mataix Verdú”, Biomedical Research Centre, University of Granada, Avda. del Conocimiento s.n, 18100, Armilla, Spain

^b Department of Genomic Medicine, GENYO: Centre for Genomics and Oncology (Pfizer-University of Granada and Andalusian Regional Government), PTS Granada, 18016, Spain

^c Department of Nutrition and Bromatology, University of Granada, 18071, Granada, Spain

^d Department of Clinical Sciences, Polytechnic University of Marche, Ancona, 60131, Italy

^e Department of Biochemistry, Faculty of Sciences, King Abdulaziz University, Jeddah, Saudi Arabia

^f Research Group on Foods, Nutritional Biochemistry and Health, Universidad Europea del Atlántico, Isabel Torres, 21, 39011, Santander, Spain

^g Department of Periodontology, Dental School, University of Seville, C/Avicena, s/n, 41009, Seville, Spain

^h International Joint Research Laboratory of Intelligent Agriculture and Agri-products Processing, Jiangsu University, Zhenjiang, China

ⁱ Sport and Health Research Centre, University of Granada, C/. Menéndez Pelayo 32. 18016 Armilla, Granada, Spain

ARTICLE INFO

Handling Editor: Dr. Jose Luis Domingo

Keywords:

Alzheimer disease
DAF-16/FOXO
HSP-16.2
IIS pathway
RNAi
SKN-1/NRF2

ABSTRACT

Olive tree-derived products have been associated with numerous benefits for health. The aim of the present study was to characterize an olive leaf extract enriched in oleuropein (OLE) concerning phenolic content and profile as well as antioxidant capacity. Short-term and long-term toxicity, including oxidative stress, was *in vivo* evaluated in the experimental model *Caenorhabditis elegans*. Moreover, the potential therapeutic effect of the extract against A β induced- and tau protein induced-toxicity was also evaluated in *C. elegans*. OLE treatment did not exert toxicity. On the contrary, the extract was able to ameliorate oxidative stress and proteotoxicity related to A β and tau aggregation. The potential molecular mechanisms present behind the observed results explored by RNAi technology revealed that DAF-16/FOXO and SKN-1/NRF2, elements of the insulin insulin-like signalling pathway, as well as HSP-16.2 overexpression were involved.

1. Introduction

Olive tree (*Olea europaea*) leaves are considered as a waste from the olive grove, which are discarded in two stages: during the pruning process and as a result of the mechanical harvesting of the olive fruit (Espeso et al., 2021). It has been estimated that the total amount of olive leaves that could be gathered in Spain alone is around 750,000 tons per year (Manzanares et al., 2017). Because of this production magnitude,

this by-product should be re-used, promoting the circular economy. Olive leaf has been used in traditional medicine since it is a valuable source of bioactive compounds (Romani et al., 2019). The most predominant compound in the olive leaf extract is the oleuropein. The presence of this secoiridoid is the reason for the characteristic bitter taste of olive cultivars (Acar-Tek and Ağagündüz, 2020). Oleuropein first is transformed into its aglycone form, and then into hydroxytyrosol, together with glucose and elenolic acid (Romani et al., 2019). The

* Corresponding author. Department of Physiology, Institute of Nutrition and Food Technology “José Mataix Verdú”, Biomedical Research Centre, University of Granada, Avda. del Conocimiento s.n, 18100, Armilla, Spain.

** Corresponding author. Sport and Health Research Centre, University of Granada, C/. Menéndez Pelayo 32. 18016 Armilla, Granada, Spain.

E-mail addresses: crissg@ugr.es (C. Sánchez-González), jquiles@ugr.es (J.L. Quiles).

¹ These authors contributed equally to this manuscript.

positive health effects of olive leaves and their compounds have been extensively demonstrated. Benefits concerning blood pressure, inflammatory status, serum lipid profile (Lockyer et al., 2017) and glycaemia (Acar-Tek and Ağagündüz, 2020; Al-Azzawie and Alhamdani, 2006) have been attributed to them, as well as antioxidant (Acar-Tek and Ağagündüz, 2020; Al-Azzawie and Alhamdani, 2006), cardioprotective (Wu et al., 2018) and anticancer (Mijatovic et al., 2011) effects. Furthermore, olive biophenols (Omar et al., 2018) have demonstrated interference with the amyloid aggregation path *in vitro* and, for oleuropein, also *in vivo* (Leri et al., 2019; Omar et al., 2018).

The increase of the incidence of neurodegenerative disorders such as dementias poses a severe challenge for the society and the healthcare system. Alzheimer's disease (AD) is the most common form of dementia, which contributes to 60–70% of the cases (World Health Organization, 2021a). Among all the diseases, AD and other dementias are the seventh leading cause of death globally (World Health Organization, 2020) and the second one in high-income countries (World Health Organization, 2020). Moreover, it is considered as one of the major causes of disability and dependency in older people (World Health Organization, 2021a), which leads to high physical, psychological, social and economic impacts (World Health Organization, 2021a). Currently, more than 55 million people live with dementia worldwide, and there are nearly 10 million new cases every year. As the proportion of older people in the population is increasing in nearly every country, this number is expected to rise to 78 million in 2030 and 139 million in 2050 (World Health Organization, 2021b). AD is a proteinopathy characterized by accumulation of hyperphosphorylated Tau and β -amyloid together with an oxidative stress increase among other features (Cordero et al., 2018; Quiles et al., 2020). Regarding the disease etiology, genetics and environmental factors are involved in this multifactorial pathology. Among them, the main modifiable risk factor is the diet (Caruso et al., 2021; Godos et al., 2020). Numerous studies have associated a neuroprotective effect with the intake of foods included in the Mediterranean Diet (Berti et al., 2018) such as the virgin olive oil and its bioactive compounds (Berr et al., 2009; Robles-Almazan et al., 2018).

The increase of AD incidence along with the population aging and the lack of effective pharmacotherapy to counteract the pathology have raised the scientific community interest in the search of compounds able to prevent, delay or treat the AD. In this sense, there is a strong need for the development of new tools and the olive leaf, and its compounds could be a promising and excellent approach. According to that, the aim of the present research was to investigate an olive leaf extract enriched in oleuropein that has been processed according to the European Pharmacopoeia (European Pharmacopoeia, 2007). This extract has been authorized to be used as an ingredient for nutritional supplements in human nutrition. Firstly, the characterization in terms of antioxidant capacity and polyphenols profile was made. Moreover, *Caenorhabditis elegans* was used to evaluate *in vivo* toxicity of the extract. This model was also used to evaluate the potential therapeutic effect of the novel formulation against AD-related proteinopathies such $A\beta$ induced- and tau protein induced-toxicity as well as to describe the molecular basis of the protective effects observed.

2. Materials and methods

2.1. Chemicals and reagents

Reagents were purchased from Thermo Fisher (Waltham, Massachusetts, USA), Sigma-Aldrich (St. Louis, Missouri, USA), Merck (Darmstadt, Germany) or Roche (Basel, Switzerland). All reagents were of analytical grade and double distilled deionized water was obtained from a Milli-Q purification system from Millipore (Milford, MA, USA).

2.2. Extract preparation

Dry extract from *Olea Europaea* leaves enriched 40% in oleuropein

(OLE) was a kind gift by Natac (Madrid, Spain). The dry extract was directly diluted in a solution composed of ethanol/Milli-Q water (25:75, v/v) for its use. This extraction medium was experimentally calculated to use the lowest concentration of ethanol to solubilize OLE with no toxicity for the experimental model. One-hundred $\mu\text{g}/\text{mL}$ of extract was used in most of the experiments with worms. (European Pharmacopoeia, 2007). Fig. S1 present a certificate of analysis in Spanish provided by the company. This analysis certifies that the content in oleuropein of the extract is a 43.68%.

2.3. Total phenolic and flavonoids content analysis

Total phenolic content of the OLE was measured by the Folin-Ciocalteu method (Singleton et al., 1999). Briefly, samples were reacted for 5 min with the Folin-Ciocalteu reagent. Next, sodium carbonate (Na_2CO_3) was added to the mixture and incubated for 2 h at room temperature. Gallic acid was used as standard, and the absorbance was measured at 760 nm. Phenolic profile was also determined by LC-MS to validate that the extract was mainly rich in oleuropein (Fig. S2 and Fig. S3). The determination of flavonoids content was performed as previously described (Navarro-Hortal et al., 2021). In this context, samples were reacted with NaNO_2 for 6 min and then, were incubated with AlCl_3 for 5 min. Next, NaOH was added and immediately the absorbance was read at 510 nm. Catechin was used as standard. For both analyses, a Synergy Neo2 microplate reader (Biotek, Winooski, Vermont, U.S.A.) was used to measure the absorbances. Every determination was carried out at least three times. The results are expressed as mg of gallic acid equivalent/g of dry extract and mg of catechin equivalent/g of dry extract for total phenolic and flavonoid content, respectively.

2.4. Total antioxidant capacity

Total antioxidant capacity of the OLE was assessed by three different methods: ABTS, DPPH and FRAP. First, ABTS assay was made following the protocol described by Re et al. (1999), which is based on the reduction of the free radical 2,2'-azinobis(3-ethylbenzothiazoline-6-sulfonic acid) by the antioxidants present in samples. The absorbance values were measured at 734 nm. Next, a DPPH assay was made following the protocol described by (Kumaran and Karunakaran, 2007). This test is based on the colorimetric measurement of the free radical 2,2-diphenyl-1-picryl-hydrazyl-hydrate (DPPH) reduction which is progressively lost when it is reduced by the antioxidant compounds of the samples. The absorbance was measured spectrophotometrically at 517 nm of wavelength. For the FRAP assay, the protocol described by Deighton et al., was followed. This assay evaluates the ability of the sample to reduce the ferric to ferrous ion. The absorbance when the iron, complexed with 2,4,6-tripyridyl-s-triazine (TPTZ), changes its color, was measured at 593 nm (Deighton et al., 2000). A Synergy Neo2 microplate reader (Biotek, Winooski, Vermont, U.S.A.) was used to measure the absorbances. Every determination was performed at least three times. Results are expressed as mM of trolox equivalents/g dry extract.

2.5. *Caenorhabditis elegans* strains and maintenance

Caenorhabditis elegans strains used in this work were N2 Bristol (wild type), CL4176 (dvIs27 [myo-3p:A-Beta (1–42):let-851 3'UTR] + rol-6 (su1006) X), CL802 (smg-1(cc546) I; rol-6(su1006) II), BR5706 (bKIs10 [aex-3p:hTau V337M + myo-2p:GFP]), LD1 ([ldIs7 [skn-1b/c:GFP + rol-6(su1006)], TJ356 (zIs356[daf-16p:daf-16a/b:GFP + rol-6(su1006)], TJ375 (gps1[hsp-16.2:GFP]), CF1553 (mu1s84[pAD76(sod-3:GFP) + rol-6(su1006)]) and CL2166 (dvIs19 [(pAF15)gst-4p:GFP:NLS] III). All strains were routinely maintained in an incubator (VELP Scientifica FOC 120 E, Usmate, Italy) at 20 °C, except CL4176 and CL802, which were maintained at 16 °C. Worms were grown on nematode growth medium

(NGM) agar plates with *Escherichia coli* OP50 as food source, according to standard protocols. The worm strains and the bacteria were acquired from the Caenorhabditis Genetics Center (Minneapolis, MI, USA). Age-synchronized animals were obtained by isolating embryos from gravid hermaphrodites using a bleaching method.

2.6. Lethality test

OLE acute toxicity assay was performed in wild-type N2 synchronized L4 larvae. In this context, age-synchronized worms were placed in NGM plates until L4 larvae state. At this moment, L4 worms were placed in plates which contained increasing concentrations of the extract dissolved in NGM (0, 0.1, 1, 10, 100, 1000 µg/mL) without food. After 24 h, nematodes were scored as live or dead using a Motic dissecting microscope (Motic Inc., LTD., Hong Kong, China). Worms were considered dead when there was no response to repeated touches with platinum wire. At least, three independent assays for each concentration were made and the experiment was performed in triplicate with a minimum of 5 worms per plate. Results were expressed as percentage of survival in 24 h. The non-lethal submaximal concentration (100 µg/mL) was selected for further experiments.

2.7. Pharyngeal pumping assay

Worm metabolism was assessed by pharyngeal pumping assay in wild-type N2 synchronized young adults. Briefly, OLE was dissolved until a final concentration of 100 µg/mL in NGM plates. Then, worms were incubated at 20 °C on *E. coli* sown plates with or without the treatment for 96 h. Next, worms were moved to different NGM plates to evaluate the number of contractions per minute of the terminal bulb of the pharynx using a Motic microscope (Motic Inc. LTD. Hong Kong, China). The experiment was performed three times and ten worms per group were evaluated (n = 10). Results are expressed as the mean number of contractions per minute.

2.8. Growth test

The effect of the OLE on worm developments was carried out similarly as described for the pharyngeal pumping assay. Briefly, four-day-old worms from treatment or control groups were photographed on a microscope (Motic Inc., LTD. Hong Kong, China) and the pictures were used to measure the body lengths using Motic Images Plus 3.0 (Motic Inc., LTD. Hong Kong, China). A minimum of three replicates were carried out with 40 worms per each one. The results are expressed as the mean of body length of worms.

2.9. Reproduction and fertility test

The effect of OLE on worm fertility and egg viability was carried out in L4 aged-synchronized N2 worms. In this context, age-synchronized worms were placed in NGM plates until L4 larvae state. At this moment, L4 worms were individually placed in 24 well plates containing or not the OLE dissolved in NGM (100 µg/mL) with *E. coli* OP50 as a source of food. After 24 h, worms from both groups were moved to a different non-treated NGM 24 well plate seeded with bacteria. Worms were continuously moved every day until they stopped laying eggs. For every single worm, eggs were counted the same day of adult removal and the larvae number were counted the day after by using a dissection microscope (Motic Inc., LTD. Hong Kong, China). At least 15 worms were used per group and the experiment was repeated at least three times. Results are expressed as the mean of the total number of eggs or larvae per group.

2.10. Lifespan analysis

Lifespan analysis was assessed to evaluate long-term toxicity of the

extract. OLE was dissolved until a final concentration of 100 µg/mL in fresh NGM plates. Then, 120 aged-synchronized worms were lifelong grown from embryos at 20 °C on supplemented or not supplemented plates and with a bacterial lawn until the last worm died. The day one of adulthood was considered as the first day of the experiment. Worms were daily transferred to fresh plates containing or not the extract to separate larvae from adults and to avoid worm starving. Animal survival was scored every day. Death was assumed when there was no response to mechanical stimulus. The worms dragged out of the dish or with extruded internal organs were considered as censored. Results are presented as a Kaplan-Meier survivorship curve.

2.11. Intracellular reactive oxygen species (ROS) content under induced oxidative stress conditions

In vivo ROS content was measured in worms by using the 2',7'-Dichlorofluorescein Diacetate (DCFDA) method, as previously described by Navarro-Hortal and coworkers (Navarro-Hortal et al., 2021). Briefly, synchronized embryos were lifelong cultured in bacteria seeded NGM plates with or without 100 µg/mL of the OLE for 48 h at 20 °C. Next, worms were washed three times with M9 buffer to remove bacteria. To induce oxidative stress, collected worms were incubated or not with 2.5 mM of 2,2'-azobis-2-amidinopropane dihydrochloride (AAPH) for 15 min at 20 °C. Then, AAPH was removed from the worms with 3 times M9 washed. Finally, worms were incubated with 25 µM of DCFDA for 2 h at 20 °C. This dye can penetrate through the cell membrane and emits fluorescence when it reacts with free radicals. The intensity of fluorescence was measured using a COPAS BioSorter® flow cytometer (Union Biométrica, Belgium, Europe). Results are expressed as the mean of the fluorescence intensity, which is related to the ROS content (AU). A minimum of three replicates were carried out with at least 180 worms per group and experiment.

2.12. Amyloid-β toxicity induced-paralysis test

Paralysis assay was performed by using CL4176 strain, a temperature sensitive transgenic strain that expresses human amyloid β₁₋₄₂ peptide in muscle cells. In this context, animals were incubated for 48 h at 16 °C from embryos on NGM containing or not 100 µg/mL of the OLE. To initiate the β-amyloid (Aβ) induced paralysis, worms were temperature-up-shifted from 16 to 25 °C. After 20 h, paralysis was scored at 2 h intervals until 32h. The strain CL802 was used as negative control in the assay. Nematodes were scored as paralyzed when there was no response to repeated touches with platinum wire. The experiment was performed in triplicate with, at least, 20 worms per group. Results are expressed as percentage (%) of non-paralyzed worms.

2.13. Amyloid-β aggregate staining

To visualize Aβ aggregates, worms of the CL4176 strain were stained with Thioflavin T. Worms used in Thioflavin T staining were grown as described for the paralysis assay. In this context, after 26 h of temperature raised from 16 °C to 25 °C on paralysis assay, worms were collected and washed 3 times with M9 buffer. First, a fixer solution (4% paraformaldehyde/M9 buffer, pH 7.4) was used to fix worms at 4 °C. After 24 h, worms were permeabilized at 37 °C with a solution made with 5% fresh β-mercaptoethanol, 1% Triton X-100 and 125 mM Tris (pH 7.4) for 24 h. Next, permeabilized solution was removed with 2 washed with M9 and worms were stained with 0.125% Thioflavin T in 50% ethanol for 30 min. Finally, Thioflavin T excess was removed with sequential ethanol washes (50%, 75%, 90%, 75%, and 50% v/v) for 2 min each one. Finally, stained worms with Thioflavin T were observed under a Nikon epi-fluorescence microscope (Eclipse Ni, Nikon, Tokyo, Japan) and images were acquired at 40× magnification using the GFP filter with a Nikon DS-Ri2 camera (Tokyo, Japan). CL802 were considered as negative control and untreated CL4176 were the positive

control.

2.14. Locomotive behavior analysis related to tau proteotoxicity

To evaluate an extensive field of the pathophysiology of the AD, we analyze the effect of the OLE in behavior parameters in a *C. elegans* model of tauopathy. BR5706 strain shows a constitutive pan-neuronal expression of pro-aggregant human Tau protein which results in the deposition of aggregates and locomotion defects mainly noted from day one of adulthood. In this context, BR5706 worms were incubated at 20 °C from eggs on NGM containing or not 100 µg/mL of the extract for 72h. Then, animals were forced to swim to stimulate worm movement. For this purpose, at least 50 worms were transferred to a slide with a drop of M9 and worm movement was recorded, tracked, and analyzed with WormLab Imaging System (MBF Bioscience, Williston, Vermont, EE. UU). The swimming speed, wavelength and wavelength dynamic amplitude were evaluated as representative parameters of locomotive behavior. The experiment was carried out in triplicate.

2.15. Expression analysis of DAF-16/FOXO, SKN-1/NRF2, HSP-16.2, GST-4 and SOD-3 in green fluorescence protein (GFP)-reporter transgenic strains

To deepen the molecular mechanisms operating under the observed effects of the OLE, transgenic strains with GFP-reporter for dauer formation (DAF)-16/FOXO, transcription factor skinhead (SKN)-1/NRF2, heat shock protein 16.2 (HSP 16.2), glutathione S-transferase (GST)-4 and superoxide dismutase (SOD)-3 were used. LD1 worms present GFP-reporter of SKN-1/NRF2 which is present in ASI chemosensory neurons in a constitutive way and migrates to cell nuclei in response to oxidative stress. TJ356 worms present a GFP-reporter of DAF-16/FOXO and the translocation of this gene to the cell nucleus can be observed by fluorescence microscopy. HSP-16.2 gene expression was evaluated in the anterior pharynx bulb of the transgenic strain TJ375 which becomes activated under oxidative stress. GST-4 is also fused with GFP on the whole body of CL2166 similarly with SOD-3 protein is expressed in the transgenic CF1553.

For all gene expression experiments with the GFP-reporter strains, worms were grown on plates with or without the OLE at 100 µg/mL for 48 h. Next, animals were moved to slides and immobilized with sodium azide (1M). Nikon epi-fluorescence microscopy (Eclipse Ni, Nikon, Tokyo, Japan) was used to catch worm images using the GFP filter fitted with a Nikon DS-Ri2 camera (Tokyo, Japan). Pictures were taken at 10× magnification except for the TJ375 strain which was 40X. NIS-Elements BR software (Nikon, Tokyo, Japan) was used to analyze images and the background signal was subtracted from all readings. A semi-quantitative scale was used for the TJ356 strain, assigning the value '1' to worms with cytosolic expression of DAF-16:GFP, '2' to the intermediate status, and '3' to the nuclear location. SKN-1:GFP fluorescence intensity was measured in the gut area below the pharynx on LD1 worms. Anterior area of the pharyngeal bulb was measured to analyze HSP-16.2:GFP expression in TJ375 worms. Finally, the whole worm body was measured to analyze fluorescence intensity related to SOD-3:GFP and GST-4:GFP expression in CF1553 and CL2166 worms, respectively. Experiments were performed in triplicate, with at least 20 worms per experiment and group.

2.16. RNAi experiments by feeding

For the RNAi experiments, *E. coli* HT115 expressing SKN-1/NRF2, HSP 16.2 (Sources BioScience, Nottingham, UK), DAF-16/FOXO, SOD-2 and SOD-3 (Cultek SL, Madrid, Spain) dsRNA were seed on NGM plates containing 1 mM Isopropyl β-D-1-thiogalactopyranoside (IPTG) and 25 µg/mL carbenicillin. Next, age-synchronized L3-L4 worms (F0) grown in standard conditions were moved to RNAi plates for the specific gene until the second day of adulthood (fertile age). Then, embryos (F1) were

isolated from gravid hermaphrodites using a bleaching method and placed into RNAi plates for the specific gene containing or not the extract and used for RNAi experiments. Once F1 embryos of CL4176 and BR5706 were obtained, the paralysis assay and locomotive behavior test with RNAi technology followed the protocols shown above for the respective test. F1 worms of the CL4176 and BR5706 were used for RNAi experiments to deepen the molecular mechanisms operating under the observed effects of the extract on amyloid-β toxicity induced-paralysis test and tau toxicity-related locomotive behavior tests, respectively.

2.17. Verification of the RNAi effect in GFP-reporter transgenic strains

To verify whether an RNAi specific gene was effective for the particular gene inhibition in RNAi experiments, F1 worms of LD1, TJ356, CF1553 and TJ375 F1 exposed or not to their specific RNAi inhibitor were used. Once F1 embryos of the mentioned strains above were obtained, verification RNAi experiments were made according to GFP-reporter transgenic strains experiment protocols.

2.18. Statistical analysis

Kolmogorov-Smirnov test was used to study the normality of the variables as well as the Levene test was used to study the homogeneity of variance. For normally distributed variables, the T-student test was employed. Non-normally distributed variables were analyzed by non-parametric tests (Kruskal-Wallis and Mann-Whitney-U). Data are expressed as mean ± SEM from at least 3 independent experiments unless otherwise stated. Significance was considered for $P < 0.05$. For lifespan curves, the Log-Rank test was used to evaluate the differences among survival distributions of cohorts. Statistical analysis was performed by SPSS 24.0 (IBM, Armonk, NY, USA).

3. Results

3.1. Total phenolics content, phenolics profile, total flavonoids content and total antioxidant capacity of OLE

Table 1 presents data on total phenolics content, total flavonoids and total antioxidant capacity measured by three different methods of OLE. Figs. S2 and S3 show phenolics profile of the OLE analyzed by LC-MS. Quantitative analysis provided by supplier certified a concentration in oleuropein in our extract sample of 43 mg/100 mg.

3.2. Toxicological characterization of oleuropein rich extract

As a first approach to the *in vivo* effects of the olive leaf oleuropein-rich extract OLE, different tests were used to evaluate the toxicity in *C. elegans*. First, oleuropein rich extract short-term toxicity was evaluated by the 24h-lethality test. As shown in Fig. 1A, all tested concentrations were non-lethal for the exposed worms, with a survival percentage near to 100% in every dosage. According to these results, non-lethal submaximal concentration (100 µg/mL) of extract was selected for the rest of the experiments. Subsequently, pharyngeal pumping (Fig. 1B) and growth (Fig. 1C) were evaluated as an overview

Table 1

Total phenolics content, total flavonoids content and total antioxidant capacity of the *Olea Europaea* leaves extract 40% rich in oleuropein (OLE).

Parameter	Mean ± SEM
Total phenolics content (mg galic/g extr)	212.1 ± 13.9
Total flavonoids content (mg catechin/g extr)	388.1 ± 34.7
FRAP (mM trolox/g extr)	3.5 ± 0.2
DPPH (mM trolox/g extr)	2.8 ± 0.1
ABTS (mM trolox/g extr)	2.3 ± 0.2

ABTS:2,2'-azinobis (3-ethylbenzothiazoline-6-sulfonic acid); DPPH: 2,2-diphenyl-1-picryl-hydrazyl-hydrate; FRAP: Ferric Reducing Antioxidant Power.

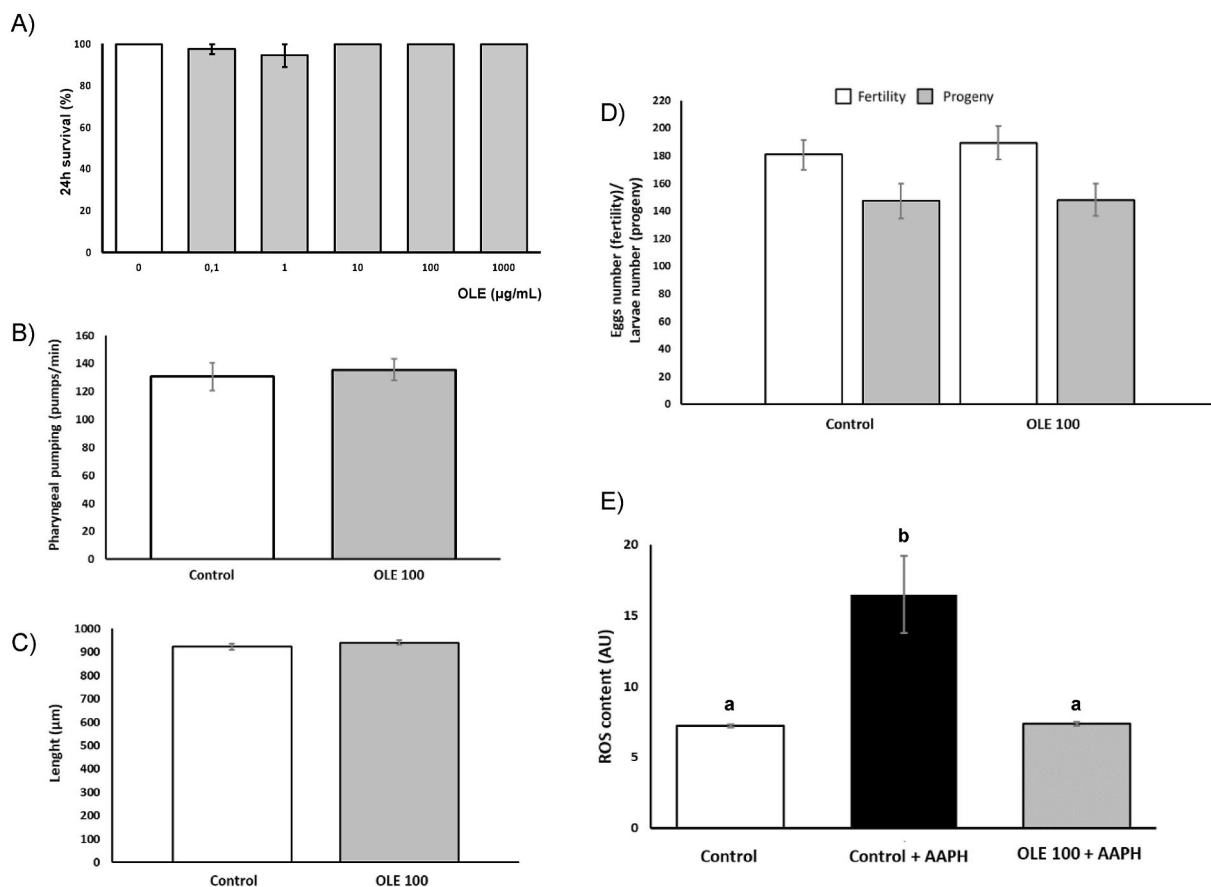


Fig. 1. Short-term *in vivo* toxicity characterization of the oleuropein rich-olive leaf extract (OLE) in the *Caenorhabditis elegans* wild type N2 strain. A) Lethality; B) Pharyngeal pumping; C) Growth; D) Reproduction and fertility; E) Reactive oxygen species (ROS) content. For each parameter, columns with different lower-case letters mean statistically significant differences ($P < 0.05$). Results are expressed as mean \pm SEM. AAPH: 2,2'-azobis-2-amidinopropane dihydrochloride.

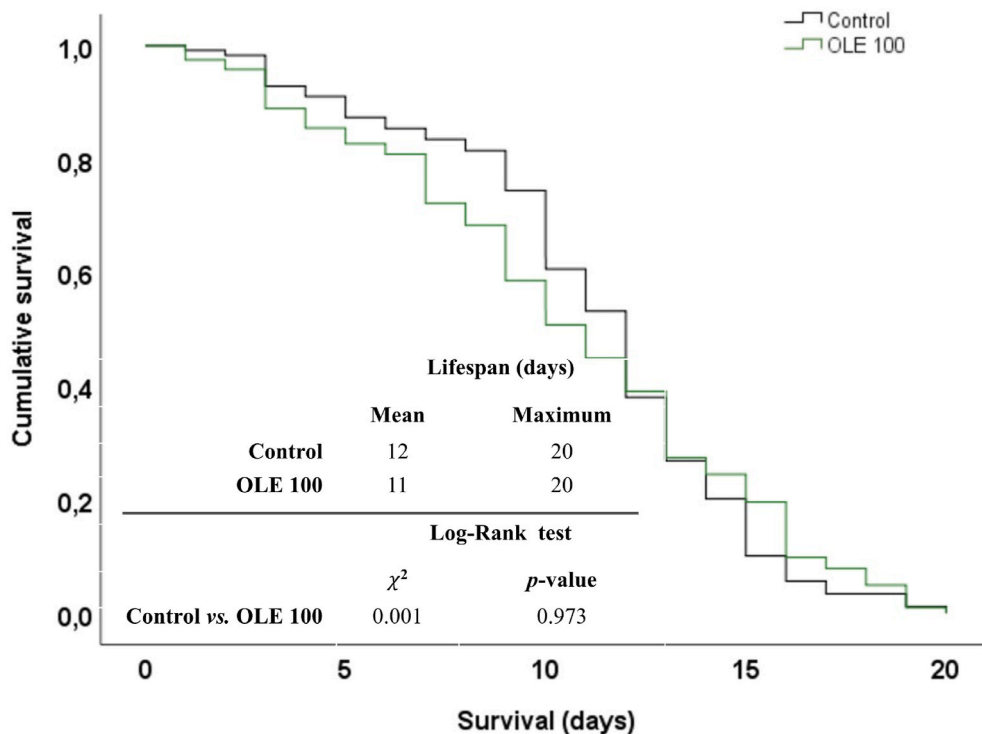


Fig. 2. Kaplan-Meier representation for the long-term *in vivo* toxicity characterization of the oleuropein rich-olive leaf extract (OLE) in the *Caenorhabditis elegans* wild type N2 strain. Mean and maximal lifespan as well as Log-Rank test are presented inside the curve.

of worm's metabolism and adequate development of nematodes. Results showed that there were no differences neither in pharyngeal pump rate nor in body length between treated and untreated worms. In the same way, as represented in Fig. 1D, treatment with the extract did not affect the ability of worms' egg-laying (reproduction) or eggs viability (progeny). Additionally, long-term toxicity of the extract was evaluated on worms using survival curves. In this context, lifespan in the worms was not affected by OLE, as presented in Fig. 2.

3.3. Effect of oleuropein rich extract on AAPH-induced oxidative stress

To test the effect of OLE regarding oxidative stress (also considered as a marker of toxicity), DCFDA was used to measure ROS after induction with the stressor AAPH. As it can be shown in Fig. 1E, AAPH induction markedly elevated ROS content in worms compared to the unexposed controls. In contrast, OLE treatment avoided AAPH related ROS enhancement, leading to similar values than those found in non-AAPH induced control group.

3.4. OLE effect on Aβ toxicity and accumulation

Paralysis test was carried out to assess the effect of OLE on Aβ toxicity using CL4176 which expresses human amyloid β₁₋₄₂ peptide in muscle cells. Results, represented in Fig. 3, showed that OLE led to a delayed paralysis in treated worms. The bigger differences on non-paralyzed worm score were obtained in the range between 24 and 28 h after the temperature upshift. Furthermore, this result was associated with the findings obtained by thioflavin T staining. Thioflavin T is a well-known reagent used to specifically dye Aβ aggregation. As shown in Fig. 3, a large number of Aβ deposits can be observed in the positive control. In contrast, extract-treated worms images reflect a clear effect of OLE, with

less accumulation of Aβ deposits. These results demonstrated that OLE treatment diminished Aβ production and/or accumulation in the Aβ human-transgenic model.

To explore the molecular mechanisms underlying the effects found in the paralysis assay, RNAi technology was used. In this context, paralysis assay was conducted as before but with worms subjected in parallel to RNAi for different genes. As can be observed in Fig. 4, the protective effect of oleuropein rich extract against Aβ-induced paralysis was partially lost in silenced DAF-16 worms. Similar results were obtained for silenced SKN-1 worms. In the same way, extract treated worms exposed to HSP-16.2 RNAi significantly reduced the non-paralyzed worm score. In contrast, the protective effect of the extract was not modified after the knockout of SOD-2 and SOD-3 enzymes by RNAi

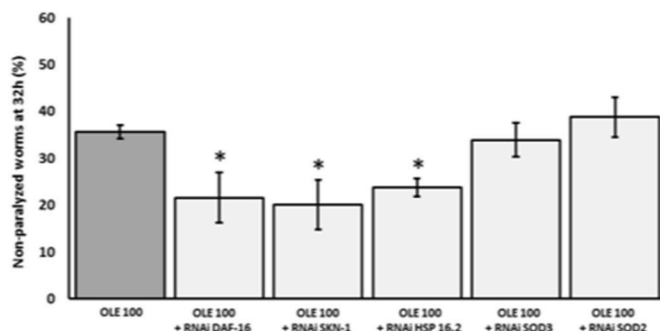


Fig. 4. Effect of the different RNAi (SKN-1, DAF-16, HSP-16.2, SOD-3 and SOD-2) on the oleuropein rich-olive leaf extract (OLE) treated CL4176 nematodes in a paralysis test. * means statistically differences (p < 0.05) with respect to OLE-treated group unexposed to RNAi. Results are expressed as mean ± SEM.

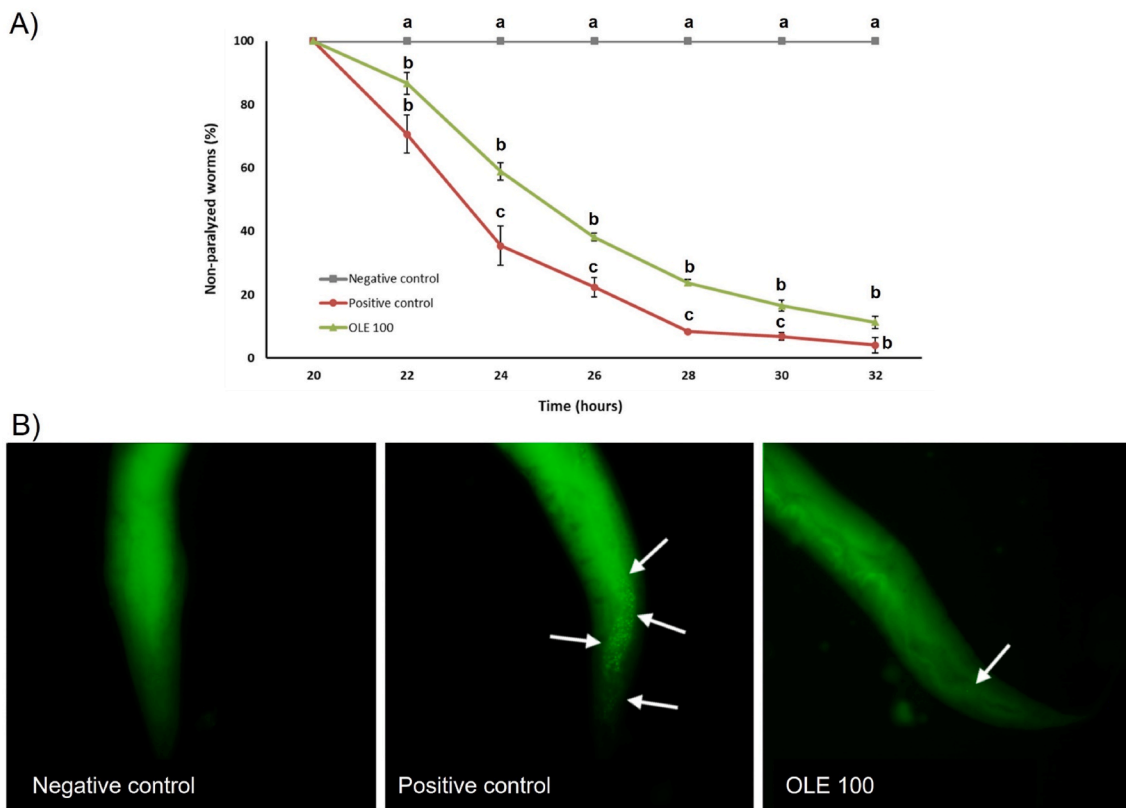


Fig. 3. Effects of the oleuropein rich-olive leaf extract (OLE) on Aβ-induced paralysis phenotype in CL4176 transgenic strain. A) Paralysis curve shown non-paralyzed CL4176 nematodes (%) since 20h after the increase of temperature. B) Thioflavin T staining shows representative images of the CL4176 nematodes collected at 26h after the increase of temperature (40× magnification). Aβ aggregates are remarked with white arrow. Different lower-case letters mean statistically differences (p < 0.05) between groups for each time. Results are expressed as mean ± SEM.

feeding.

3.5. Effect of OLE on transgenic GFP reporter strains of DAF-16, SKN-1, HSP-16.2, GST-4 and SOD-3

To test the effect of OLE on genes blocked by RNAi, transgenic strains in which the targeted gene was marked with GFP were treated with the extract and expression assessed by fluorescence microscopy. Thus, GFP fluorescence for DAF-16, SKN-1, HSP-16.2, GST-4 and SOD-3 transgenic strains after OLE treatment is presented in Fig. 5. Worms from the TJ356 strain were individually classified in cytosolic, intermediate or nuclear according to the presence of nucleation of DAF-16:GFP (Fig. 5B). As shown in Fig. 5A, the assayed dosage of OLE did not induce the nuclear translocation of the transcription factor nor increased the expression of SKN-1:GFP in the LD1 strain (activation of this transcription factor is also mediated by its nucleation (Figure C). On the other hand, CF1553 worms treated with the oleuropein rich extract increased the fluorescence intensity of SOD-3:GFP (Fig. 5A and D). In the same way, OLE increased the expression of HSP-16.2:GFP compared to untreated TJ375 worms (Fig. 5A and E). In contrast, expression of GST-4:GFP was reduced by oleuropein rich extract in comparison with untreated CL2166 worms (Fig. 5A and F).

To verify that the RNAi feeding technology was effective on different tests, specific transgenic GFP reporter strains were exposed to their respective RNAi. As shown in Fig. 6, DAF-16:GFP, SKN-1:GFP, SOD-3:GFP and HSP-16.2:GFP expression in the specific GFP reporter strain was reduced by RNAi exposure.

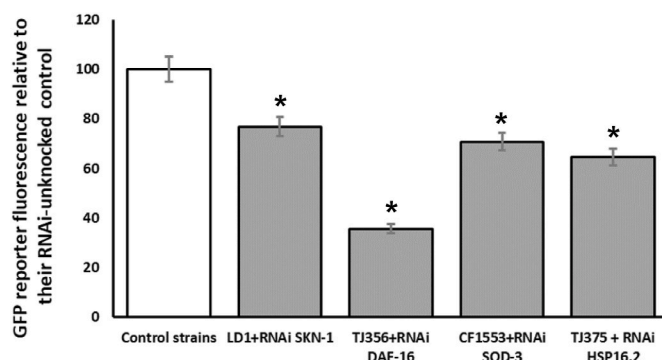


Fig. 6. Verification of the effect of RNAi in the transgenic strains LD1 (SKN-1:GFP), TJ356 (DAF-16:GFP), CF1553 (SOD-3:GFP) and TJ375 (HSP-16.2:GFP). Results are expressed as percentage with respect to the control group of the same strain without the RNAi for the specific gene. * Means statistically significant differences with the control group ($P < 0.05$).

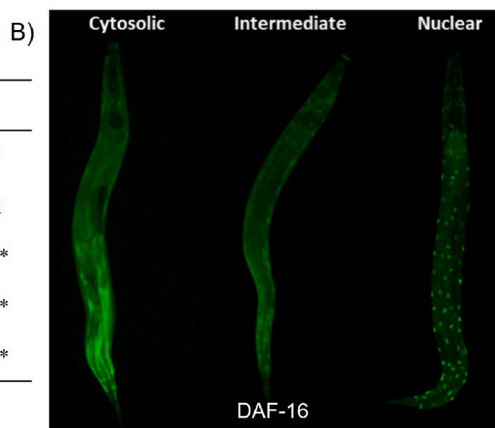
3.6. Effect of oleuropein rich extract on locomotive behavior related to tau proteotoxicity

To test more features associated with AD besides A β aggregation, tau aggregation was analyzed by investigating swimming locomotive behavior. By using the WormLab station and software, swimming speed, wavelength and wavelength dynamic amplitude parameters were chosen (Fig. 7). Swimming speed is the traveling speed of an animal

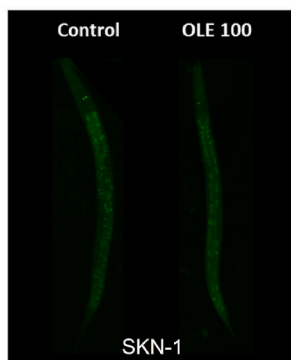
A) Quantification of the GFP expression on the different transgenic strains gene reporters treated with OLE.

	Control	OLE 100
DAF-16:: GFP nuclear expression (AU)	1.05 \pm 0.04	1.11 \pm 0.07
SKN-1::GFP expression (AU)	12.28 \pm 0.92	12.16 \pm 0.81
SOD-3::GFP expression (AU)	35.11 \pm 2.34	45.24 \pm 2.53*
HSP-16.2::GFP expression (AU)	29.41 \pm 2.22	44.82 \pm 3.01*
GST-4::GFP expression (AU)	47.04 \pm 3.32	36.88 \pm 2.66*

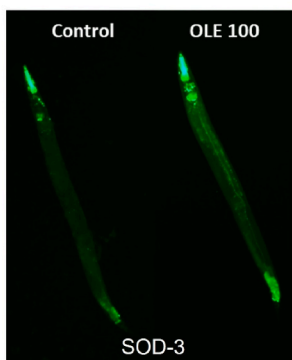
*Statistical significance ($P < 0.05$) between Control and OLE100.



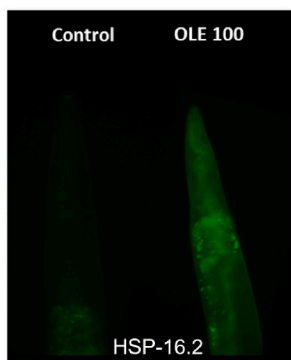
C)



D)



E)



F)

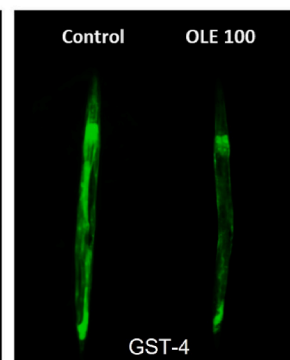


Fig. 5. Effects of the oleuropein rich olive leaf extract (OLE) on GFP-reporter transgenic strains. A) Quantification of the GFP expression on the different transgenic strains gene reporters treated with OLE. B) Illustrative images of the different status of DAF-16:GFP (cytosolic, intermediate or nuclear) in the strain TJ356 (10 \times magnification). C) Illustrative images of SKN-1:GFP expression in the strain LD1 for each group (10 \times magnification). D) Illustrative images of SOD-3:GFP expression in the strain CF1553 for each group (10 \times magnification). E) Illustrative images of HSP-16.2:GFP expression in the strain TJ375 for each group (40 \times magnification). F) Illustrative images of GST-4:GFP expression in the strain CL2166 for each group (10 \times magnification). Results are expressed as mean \pm SEM. * means statistically significant differences with the control group ($P < 0.05$).

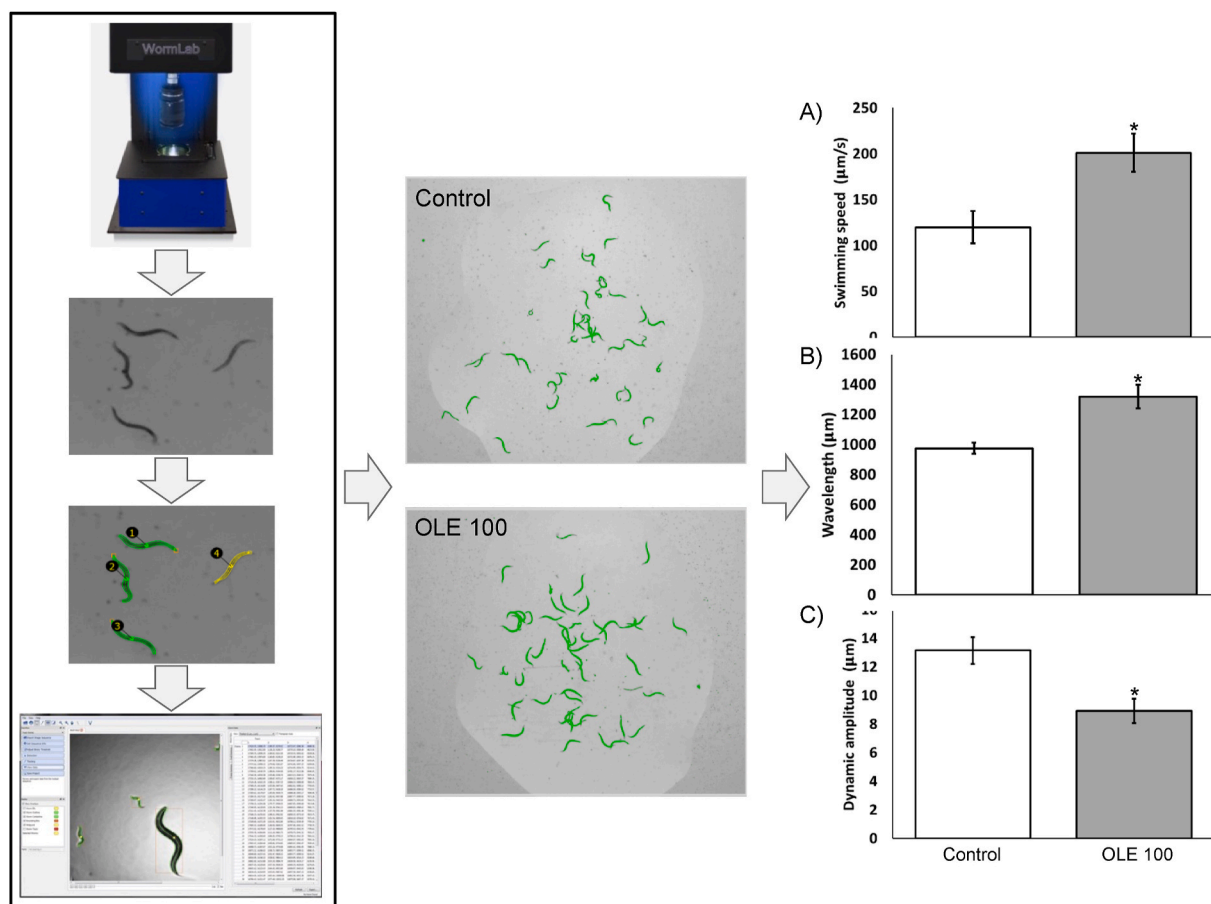


Fig. 7. Effects of OLE on Tau-induced altered locomotive behavioral phenotype in BR5706 transgenic strain. A) Swimming speed B) Wavelength. C) Dynamic amplitude/stretching effort. *Means statistically differences ($p < 0.05$) with respect to the OLE-treated group unexposed to RNAi. Results are expressed as mean \pm SEM. The picture also shows a representation of the process followed with WormLab system and software to process locomotive worm's video.

measured over a two-stroke interval, whereas wavelength determines the magnitude of the body's waviness. Furthermore, the wavelength dynamic amplitude provides an estimate of the type of body bend (deep or flat) and of the intensity of the "stretching" effort in a stroke. Overall, proaggregatory tau worms treated with OLE showed better locomotive parameters, with a higher speed and wavelength and a lower stretching effort (dynamic amplitude) compared with control groups.

To explore the molecular mechanisms underlying the effects found in the locomotive behavior assay, RNAi technology was used. In this context, the same experiment as before was conducted with the extract and subjected to RNAi for different genes (SKN-1, DAF-16, HSP-16.2, SOD-3 and SOD-2). As can be observed in Fig. 8, the protective effect of OLE against locomotive alterations related to tau-neurotoxicity was modified in different knockout worms. Thus, swimming speed was reduced in all studied knockout extract-treated worms except in those knocked out SOD-3 worms (Fig. 8A). Concerning the worm's wavelength, the waviness was reduced in all knockout extract-treated worms studied (Fig. 8B). Finally, the stretching effort was increased in all studied knockout extract-treated worms except in knockout SOD-3 worms (Fig. 8C).

4. Discussion

Olive leaves consumption has been associated with various health benefits including protection against neurodegenerative diseases in preclinical models and in humans (Giacometti and Grubić-Kezele, 2020; Lockyer et al., 2017; Sarbishegi et al., 2018). Those effects could be attributed to their great phytochemicals content, especially oleuropein

(Romani et al., 2019; Vogel et al., 2014). UPLC-QTOF-MS/MS methodology was used to confirm that the concentrated extract was mainly rich in oleuropein and, with a small amount of its derivative hydroxytyrosol. These data would serve to assign the results observed in the present investigation to the high content of oleuropein of the extract used in this study. Concerning total phenolic content, results were similar to those found by Orak et al., in different methanolic olive leaves extracts from Turkey and Italy (Orak et al., 2019). However, OLE showed higher values for the three different methods of antioxidant capacity (ABTS, FRAP and DPPH) (Nicolì et al., 2019; Orak et al., 2019; Zaïri et al., 2020) as well as higher total flavonoids content (Nicolì et al., 2019). In contrast, Zaïri et al. showed that an aqueous olive leaf extract from Turkey presented higher phenolic and flavonoid content compared to our results (Zaïri et al., 2020). Those differences could be attributed to the variations in the geographic location, stage of harvesting, storage conditions as well as different extraction procedures and solvents used.

C. elegans is a very useful model to investigate the effect of food by-products in some biomedical research areas such as toxicology. To our knowledge, evidence about the olive leaves extract toxicity on *C. elegans* is very limited and this is the first investigation providing evidence on a 40% concentrated oleuropein extract concerning toxicity and AD features. According to literature, Luo et al. showed that food clearance (a similar form to measure worm metabolism/pharyngeal pumping) was not reduced (400 µg/mL) or even increased (300, 500 and 600 µg/mL) in nematodes treated with a methanolic olive leaves extract. In the same way, egg laying was increased in worms treated with 400 µg/mL of the extract (Luo et al., 2019). In the present research, pharyngeal pumping as well as reproduction and fertility tests were not affected by a lower

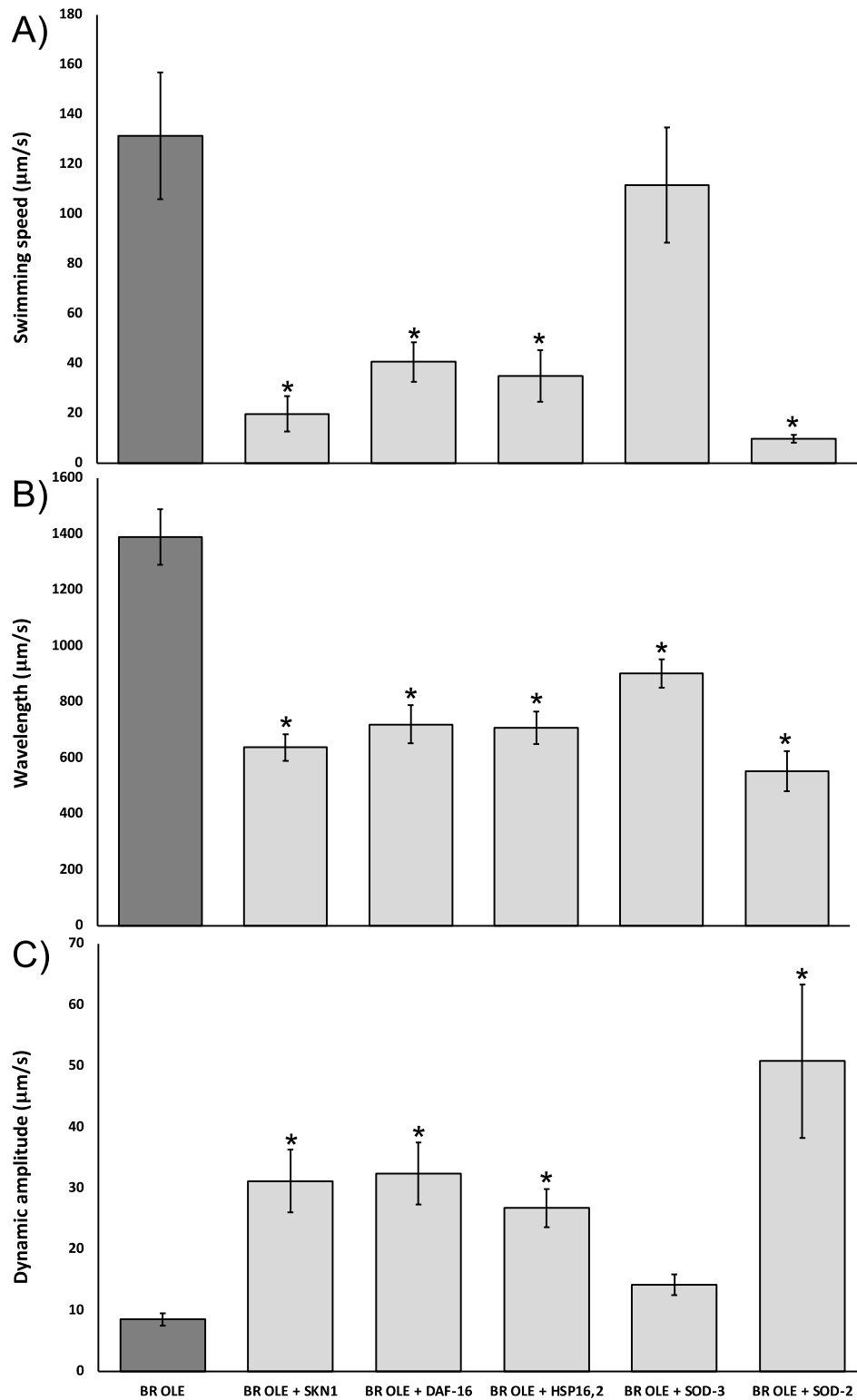


Fig. 8. Effect of the different RNAi (SKN-1, DAF-16, HSP-16.2, SOD-3 and SOD-2) on OLE treated BR5706 nematodes in the locomotive behavioral test. A) Swimming speed B) Wavelength. C) Dynamic amplitude/stretching effort. *Means statistically differences ($p < 0.05$) with respect to the OLE-treated group unexposed to RNAi. Results are expressed as mean \pm SEM.

concentration of olive leaf treatment (100 µg/mL). In fact, OLE treatment did not exert lethality at all assayed dosages (0, 0.1, 1, 10, 100, 1000 µg/mL). Likewise, *C. elegans* has been used to study oleuropein toxicity by Feng et al. Similarly, to results from the present research,

worm length and body width were not affected by the exposure to differing concentrations (0, 21.6, 97.2, 237.6 µg/mL) of a pure oleuropein extract. In the same way, lifespan was not affected by the lowest concentration of oleuropein but was increased by the rest of dosages

(Feng et al., 2021). In the present study, lifespan was not affected by OLE which contains near to 40 µg/mL of oleuropein. These results could indicate that oleuropein-mediated effects on lifespan are dose-dependent. Overall, the fact that the oleuropein rich-olive leaf extract used in the present study did not exhibit toxicity is extremely interesting regarding the possible usefulness of the extract in the search for biomedical applications.

Therefore, once the absence of OLE toxicity was evaluated, the next step was to elucidate the effectiveness of the extract against oxidative stress (which additionally can be considered a marker of toxicity). It should be noted that oxidative stress is considered as an early and critical event of the pathobiology of the AD in worms and humans (Bonda et al., 2010; Drake et al., 2003). In this context, OLE was able to prevent ROS burst after AAPH in the N2 wild strain. Similar results were observed with 400 µg/mL of methanolic olive leaves extract which also reduced ROS content in *C. elegans* under thermal stress (Luo et al., 2019). These results are in the same line with the obtained *in vitro* by Ranieri et al. In this research, CD4 cells pretreated with 10 µg/mL of green olive leaf extract showed a notable reduction of ROS content under oxidative stress conditions (Ranieri et al., 2019). This effect could be attributed to oleuropein, the major compound present in the extract, which also showed interesting properties against oxidative damage in *C. elegans*. In this context, oleuropein treatment (97.2 and 237.6 µg/mL) increased oxidative stress tolerance in wild type strain. However, the lowest concentration (21.6 µg/mL) was not effective (Feng et al., 2021). According to results from the present study, OLE might display a positive effect on neurodegenerative diseases by its influence on oxidative stress. In fact, OLE presents an optimal formulation in comparison with those that use olive leaves or pure oleuropein extract alone, demonstrating positive results at lower doses than those mostly used in literature.

To the best of our knowledge, this is the first study carried out in *C. elegans* to determine the effect of an olive leaf extract in the AD pathogenesis. AD is the most common neurodegenerative disorder characterized by impairment of cognitive function and memory loss. AD is characterized by two histopathological hallmark lesions: the deposition of Aβ peptide and the abnormal phosphorylation of tau protein (Gao et al., 2018). Most of research has been focused on the amyloid cascade hypothesis which posits that the deposition of Aβ peptide initiates a sequence of events that lead to classic symptoms of AD. However, many experimental results indicate that Aβ-associated symptoms might occur only in the presence of tau pathology (Desikan et al., 2012). To generate a deep therapeutic characterization of OLE extract used in the present study, both pathological mechanisms on different AD *C. elegans* models have been assayed. In this context, the protective effect of the OLE against Aβ toxicity in the transgenic strain CL4176 which expresses human Aβ in muscle cells causing a progressive paralysis phenotype was investigated. According to the results, OLE avoided Aβ toxicity which led to delay of the paralysis phenotype. These results were supported by Thioflavin-T staining which confirmed that the lower Aβ toxicity was caused by a lower Aβ aggregation in treated worms. Those effects could be also attributed to oleuropein which is shown to reduce, with dose of pure oleuropein of 27 µg/mL, Aβ aggregation and toxicity in two different Aβ-inducible paralysis *C. elegans* models (Diomedea et al., 2013). Indeed, *in vitro* studies have revealed that pure oleuropein interferes with the human Aβ aggregation, skipping the appearance of toxic oligomers and promoting peptide aggregation into aggregates devoid of cytotoxicity (Luccarini et al., 2014; Rigacci et al., 2011).

In the present study, RNAi technology was used to elucidate putative mechanisms underlying therapeutic effects of the OLE concerning reduction of Aβ aggregation. The insulin/insulin-like growth factor 1 (IGF-1) signaling (IIS) pathway is an evolutionarily conserved phosphorylation cascade that is involved in numerous processes which have been linked to aging and aging-related diseases such AD (Zemva and Schubert, 2014). Thus, the role of DAF-16, which is the homolog of forkhead box transcription factor class O (FoxO) in *C. elegans* was investigated. DAF-16 acts through the canonical transcriptional target of

IIS with an important performance in the regulation of Aβ aggregation (Zečić and Braeckman, 2020; Zhi et al., 2017). Also SKN-1, which is the ortholog of mammalian nuclear factor erythroid 2-related factor 2 (Nrf-2) transcription factor for *C. elegans*, was analyzed. SKN-1 is involved in xenobiotic and oxidative stress responses which is critical in early pathogenic processes in AD (Tullet et al., 2017). Among the downstream targets, some genes were also evaluated due to involvement in the antioxidant system (SOD-2 and SOD-3) and the important role in the degradation of misfolded proteins (HSP-16.2) (Zečić and Braeckman, 2020). In this context, CL4176 worms treated with OLE were exposed to RNAi clones for DAF-16, SKN-1, SOD-2, SOD-3 and HSP-16.2 under the same experimental conditions as mentioned in the paralysis assay. According to results, DAF-16 or SKN-1 knockout worms presented greater paralysis degree than unexposed RNAi worms. These results indicate that those transcription factors are involved in the effectiveness of the OLE treatment against Aβ-induced toxicity. Among the downstream target genes studied, HSP-16.2 was also implicated in the protective effect of the extract but not SOD-2 and SOD-3.

On the other hand, the present study also evaluated the effect of OLE regarding tau induced neurotoxicity in *C. elegans*. The BR5706 strain shows a constitutive pan-neuronal expression of pro-aggregant human tau protein which results in locomotion defects. Interestingly, pro-aggregatory tau worms treated with the OLE improved their movement speed and wavelength as well as the stretching effort was lower. These results suggest that the OLE treatment was able to reduce the locomotive alterations related to tau-neurotoxicity in this *C. elegans* model of AD. Those effects could be also attributed to oleuropein which has shown to interfere *in vitro* with tau fibrillization and aggregation at a very low dosage (5.4 µg/mL) resulting in a reduction of tau toxicity (Daccache et al., 2011). In the same way, oleuropein treatment (270 µg/mL) has shown to be effective in the reduction of motor alteration related to neural and muscular proteotoxicity in two different Parkinson *C. elegans* models (Brunetti et al., 2020). To explore the molecular mechanisms observed under therapeutic effects of the OLE, RNAi technology was used in the pro-aggregant human tau protein strain. In this context, RNAi selected to knockdown genes were SKN-1, DAF-16, HSP-16.2, SOD-2 and SOD-3 to find common therapeutic pathways with Aβ-progression. DAF-16 or SKN-1 knockout worms presented a reduced locomotive behavior than unexposed RNAi worms. These results indicate that those transcription factors are involved in the effectiveness of the OLE treatment against tau proteotoxicity. Similarly, HSP-16.2 and SOD-2 were also implicated in the protective effect of the extract but not SOD-3.

Towards letting deep in the therapeutic mechanism of action of the extract, GFP-tagged reporter strains were used to identification the effect of the extract on assayed targets. OLE treatment, in the dosage used in the present study, did not induce the nuclear translocation of DAF-16 as well as SKN-1 expression. In contrast to results found in the present study, Luo et al. reported that worms treated with higher dosage of methanolic olive leaves extracts (400 µg/mL) were able to induce nuclear translocation of DAF-16 which was associated with the increasing activities of antioxidant enzymes in *C. elegans* (Luo et al., 2019). In the same way, the administration of oleuropein (237.6 µg/mL) increased the nuclear translocation of DAF-16 and SKN-1 gene expression (Feng et al., 2021). These results indicate that the dosage used in this work was not enough to induce the nuclear translocation of DAF-16 and expression of SKN-1 in the GFP reporter strains in basal conditions. Notwithstanding, the therapeutic effect observed in both AD models studied were mediated by these transcription factors which could indicate that those genes may be altered by the extract under AD related stress conditions. It should be noted that DAF-16 and SKN-1 are well-known transcription factors that regulate a number of genes, so inhibiting those master regulators could also block some downstream target genes that could have an important role in the pathogenesis of AD in *C. elegans*. In the same way, in the present study it was identified an upregulation of the SOD-3 expression in worms treated with OLE. However, the inhibition of

SOD-3 in A β and tau induced toxicity strains exhibited no effect in their respective assays, which means that OLE mediated effects against A β and tau toxicity are independent of SOD-3. Interestingly, SOD-3 encodes auxiliary and inducible MnSOD mitochondrial isoforms whereas SOD-2 encodes the major MnSOD mitochondrial isoforms in *C. elegans* (Doonan et al., 2008). In this context, worms knocked out of SOD-2 showed an impairment of locomotive behavior related to tau neurotoxicity. Melov et al. proved that null SOD-2 mice express higher levels of tau phosphorylation which was associated with an increased AD-like neocortical pathology (Melov et al., 2007). These data support the idea that the effects of OLE against tau toxicity were mediated through the reduction of mitochondrial oxidative stress, at least in part, by SOD-2. On the other hand, HSP-16.2 expression was increased by the OLE treatment. Similarly, Luo et al. reported that worms exposed to higher dosage of methanolic olive leaves extracts (400 μ g/mL) also increased HSP-16.2 expression (Luo et al., 2019). HSP-16.2 is an important element of protein homeostasis which involves highly conserved stress responses that prevent protein mismanagement. In *C. elegans*, HSP-16.2 encodes HSP-16, which directly interacts with A β peptide and interfere with oligomerization pathways, leading to reduced formation of toxic species (Ai et al., 2018; Fonte et al., 2008). In the present research, OLE treatment showed null therapeutic effect when HSP-16.2 was knocked out in the A β and tau induced toxicity test. Therefore, it is not surprising that an overexpression of HSP-16.2 could have therapeutic effects on AD. Thus, results found in the present study suggest that the therapeutic effect against AD of the OLE extract is directly related to HSP-16.2

overexpression. Finally, a reduction of the GST-4:GFP expression was also found here. GST-4 plays an important role in the detoxification of reactive oxygen species. This result could be explained due the strong antioxidant activity of the extract, particularly as a free radical scavenger. *In vitro* studies have demonstrated that numerous strong antioxidants that act as ROS scavengers are able to reduce the expression or the activity of different inducible antioxidant enzymes such as glutathione S-transferase (GST), catalase (CAT) and NADH quinone oxidoreductase (NQO-1) (Jin et al., 2016). The proof of such a feature has been established by human trials. In this context, different randomized double-blind trials have reported that the intake of oleuropein-rich extra virgin olive oil enhanced plasma glutathione as well as reduced the activity of glutathione peroxidase, without changes in the expression of genes encoding for Nrf2 (Oliveras-López et al., 2013; Perez-Herrera et al., 2013). These data suggest that OLE may act as a direct cytosolic ROS scavenger, as shown in DCFDA assay (Fig. 1E), reducing the demand for certain antioxidant enzymes such as GST-4. Taken together, OLE has demonstrated great anti-AD effects through the modulation of mitochondrial oxidative stress as well as the reduction of toxic protein aggregation *in vivo*. To highlight, OLE is allowed for human nutrition supplementation, so given the promising results obtained, it might interest to test it in further clinical assays with humans affected by AD. The dose of extract used in this study has a lower concentration of oleuropein than that used in some studies. From a supplementation point of view, the use of a low dose is interesting. However, further investigations are warranted to study whether a higher dose of extract could have an effect

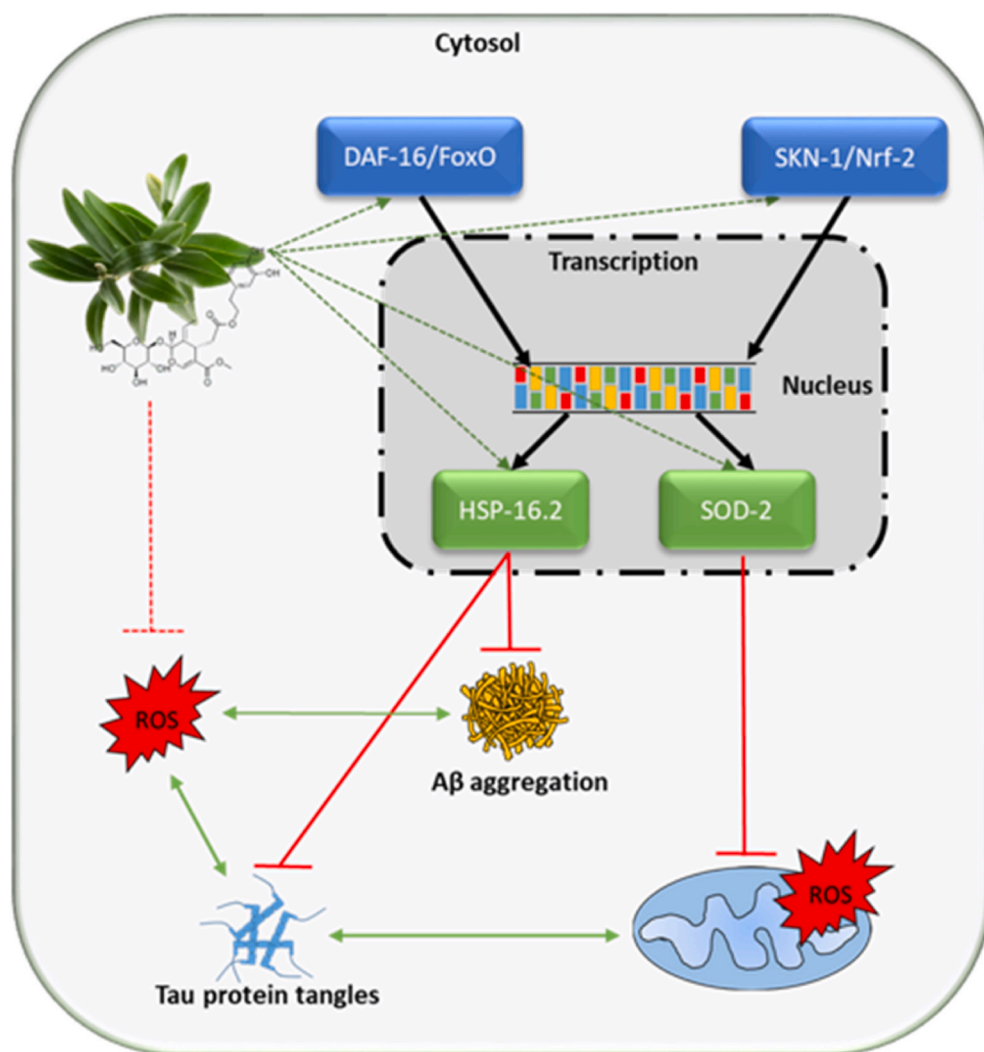


Fig. 9. Summary of the mechanisms of action of Oleuropein rich olive leaf extract (OLE) against oxidative stress and AD-related proteotoxicity in *Caenorhabditis elegans*. The extract improved markers of AD such as oxidative stress, A β aggregation as well as tau neurotoxicity in the nematode. The observed effects were mediated, at least in part, by the two master regulators DAF-16/FOXO and SKN-1/NRF2 signaling pathways. Green arrows indicate induction in the process. Red truncated lines indicate a decrease in the process. Dashed arrows indicate a direct effect of the extract. (For interpretation of the references to color in this figure legend, the reader is referred to the Web version of this article.)

on some of the gene markers studied on which the present dose has not shown such an effect.

5. Conclusions

The oleuropein rich olive leaf extract (OLE) investigated in the present study showed a high antioxidant capacity *in vitro*. OLE exerted no toxicity in the *in vivo* model *Caenorhabditis elegans*, demonstrated by short- and long-term toxicity tests. On other hand, the extract was able to improve markers of AD such as oxidative stress, A β aggregation as well as tau neurotoxicity in the nematode. The mechanisms observed concerning A β and tau accumulation as well as oxidative stress were mediated by the two master regulators DAF-16/FOXO and SKN-1/NRF2, including also a positive effect mediated by HSP-16.2. Fig. 9 summarizes the proposed mechanism of action of the extract against AD-related proteotoxicity and oxidative stress. Together, these results feature the interest of olive leaves as a source of ingredients for nutraceuticals focused on the prevention and/or treatment of several aspects related to Alzheimer's disease. Finally, a limitation when analyzing the real scope of the findings of this research should be mentioned. In this way, there is a need to investigate the effect of extracts enriched with different proportions of the active ingredient on the markers analyzed in the present study.

Formatting of funding sources

The authors gratefully acknowledge the funding support of FEDER/Junta de Andalucía-Consejería de Economía y Conocimiento, Grant B-AGR-193-UGR18. Also grant PID2019-106778RB-I00, funded by MCIN/AEI/10.13039/501100011033 FEDER "Una manera de hacer Europa".

CRedit authorship contribution statement

Jose M. Romero-Márquez: Methodology, Investigation, Writing – original draft, Preparation, Writing – review & editing. **María D. Navarro-Hortal:** Methodology, Investigation, Writing – original draft, Preparation, Writing – review & editing. **Victoria Jiménez-Trigo:** Methodology, Investigation. **Laura Vera-Ramírez:** Formal analysis, Writing – review & editing. **Tamara J. Forbes-Hernández:** Data curation, Software, Reviewing. **Adelaida Esteban-Muñoz:** Methodology, Investigation. **Francesca Giampieri:** Methodology, Validation, Writing – review & editing. **Pedro Bullón:** Visualization, Writing – review & editing. **Maurizio Battino:** Conceptualization, Visualization, Reviewing. **Cristina Sánchez-González:** Conceptualization, Data curation, Visualization. **José L. Quiles:** Conceptualization, Supervision, Writing – review & editing.

Declaration of competing interest

The authors declare that they have no known competing financial interests or personal relationships that could have appeared to influence the work reported in this paper.

Acknowledgment

María D. Navarro-Hortal and Jose M. Romero-Márquez are FPU fellows with grant reference FPU2017/04358 and FPU2018/05301, respectively, funded by MCIN/AEI/10.13039/501100011033 and FSE "El FSE invierte en tu futuro".

Appendix A. Supplementary data

Supplementary data to this article can be found online at <https://doi.org/10.1016/j.fct.2022.112914>.

References

- Acar-Tek, N., Ağagündüz, D., 2020. Olive leaf (*Olea europaea* L. Folium): potential effects on glycemia and lipidemia. *ANM* 76, 10–15. <https://doi.org/10.1159/000505508>.
- Ai, L., Yang, F., Song, J., Chen, Y., Xiao, L., Wang, Q., Wang, L., Li, H., Lei, T., Huang, Z., 2018. Inhibition of abeta proteotoxicity by paeoniflorin in *Caenorhabditis elegans* through regulation of oxidative and heat shock stress responses. *Rejuvenation Res.* 21, 304–312. <https://doi.org/10.1089/rej.2017.1966>.
- Al-Azzawie, H.F., Alhamdani, M.-S.S., 2006. Hypoglycemic and antioxidant effect of oleuropein in alloxan-diabetic rabbits. *Life Sci.* 78, 1371–1377. <https://doi.org/10.1016/j.lfs.2005.07.029>.
- Berr, C., Portet, F., Carriere, I., Akbaraly, T., Fear, C., Gourlet, V., Combe, N., Barberger-Gateau, P., Ritchie, K., 2009. Olive oil and cognition: results from the three-city study. *Dement. Geriatr. Cognit. Disord.* 28, 357–364. <https://doi.org/10.1159/000253483>.
- Berti, V., Walters, M., Sterling, J., Quinn, C.G., Logue, M., Andrews, R., Matthews, D.C., Osorio, R.S., Pupi, A., Vallabhajosula, S., Isaacson, R.S., de Leon, M.J., Mosconi, L., 2018. Mediterranean diet and 3-year Alzheimer brain biomarker changes in middle-aged adults. *Neurology* 90, e1789–e1798. <https://doi.org/10.1212/WNL.0000000000005527>.
- Bonda, D.J., Wang, X., Perry, G., Nunomura, A., Tabaton, M., Zhu, X., Smith, M.A., 2010. Oxidative stress in Alzheimer disease: a possibility for prevention. *Neuropharmacology* 59, 290–294. <https://doi.org/10.1016/j.neuropharm.2010.04.005>.
- Brunetti, G., Di Rosa, G., Scuto, M., Leri, M., Stefani, M., Schmitz-Linneweber, C., Calabrese, V., Saul, N., 2020. Healthspan maintenance and prevention of Parkinson's-like phenotypes with hydroxytyrosol and oleuropein aglycone in *C. elegans*. *Int. J. Mol. Sci.* 21, E2588. <https://doi.org/10.3390/ijms21072588>.
- Caruso, G., Torrisi, S.A., Mogavero, M.P., Currenti, W., Castellano, S., Godos, J., Ferri, R., Galvano, F., Leggio, G.M., Grosso, G., Caraci, F., 2021. Polyphenols and neuroprotection: therapeutic implications for cognitive decline. *Pharmacol. Ther.* <https://doi.org/10.1016/j.pharmthera.2021.108013>, 108013.
- Cordero, J.G., García-Escudero, R., Avila, J., Gargini, R., García-Escudero, V., 2018. Benefit of oleuropein aglycone for Alzheimer's disease by promoting autophagy. *2018 Oxid. Med. Cell. Longev.*, e5010741. <https://doi.org/10.1155/2018/5010741>.
- Daccache, A., Lion, C., Sibille, N., Gerard, M., Slomianny, C., Lippens, G., Cotelle, P., 2011. Oleuropein and derivatives from olives as Tau aggregation inhibitors. *Neurochem. Int.* 58, 700–707. <https://doi.org/10.1016/j.neuint.2011.02.010>.
- Deighton, N., Brennan, R., Finn, C., Davies, H.V., 2000. Antioxidant properties of domesticated and wild *Rubus* species. *J. Sci. Food Agric.* 80, 1307–1313. [https://doi.org/10.1002/1097-0010\(200007\)80:9<1307::AID-JSFA638>3.0.CO;2-P](https://doi.org/10.1002/1097-0010(200007)80:9<1307::AID-JSFA638>3.0.CO;2-P).
- Desikan, R.S., McEvoy, L.K., Thompson, W.K., Holland, D., Brewer, J.B., Aisen, P.S., Sperling, R.A., Dale, A.M., Alzheimer's Disease Neuroimaging Initiative, 2012. Amyloid- β -associated clinical decline occurs only in the presence of elevated P-tau. *Arch. Neurol.* 69, 709–713. <https://doi.org/10.1001/archneurol.2011.3354>.
- Diomedea, L., Rigacci, S., Romeo, M., Stefani, M., Salmona, M., 2013. Oleuropein aglycone protects transgenic *C. elegans* strains expressing A β 42 by reducing plaque load and motor deficit. *PLoS One* 8, e58893. <https://doi.org/10.1371/journal.pone.0058893>.
- Doonan, R., McElwee, J.J., Matthijssens, F., Walker, G.A., Houthoofd, K., Back, P., Matscheski, A., Vanfleteren, J.R., Gems, D., 2008. Against the oxidative damage theory of aging: superoxide dismutases protect against oxidative stress but have little or no effect on life span in *Caenorhabditis elegans*. *Genes Dev.* 22, 3236–3241. <https://doi.org/10.1101/gad.504808>.
- Drake, J., Link, C.D., Butterfield, D.A., 2003. Oxidative stress precedes fibrillar deposition of Alzheimer's disease amyloid β -peptide (1–42) in a transgenic *Caenorhabditis elegans* model. *Neurobiol. Aging* 24, 415–420. [https://doi.org/10.1016/S0197-4580\(02\)00225-7](https://doi.org/10.1016/S0197-4580(02)00225-7).
- Espeso, J., Isaza, A., Lee, J.Y., Sørensen, P.M., Jurado, P., Avena-Bustillos, R. de J., Olaizola, M., Arboleya, J.C., 2021. Olive leaf waste management. *Front. Sustain. Food Sys.* 5, 162. <https://doi.org/10.3389/fsufs.2021.660582>.
- European Pharmacopoeia, 2007. Olive leaf dry extract. In: *PHARMEUROPA*, 19.3, pp. 510–511.
- Feng, S., Zhang, C., Chen, T., Zhou, L., Huang, Y., Yuan, M., Li, T., Ding, C., 2021. Oleuropein enhances stress resistance and extends lifespan via insulin/IGF-1 and SKN-1/Nrf2 signaling pathway in *Caenorhabditis elegans*. *Antioxidants* 10, 1697. <https://doi.org/10.3390/antiox10111697>.
- Fonte, V., Kipp, D.R., Yerg, J., Merin, D., Forrestal, M., Wagner, E., Roberts, C.M., Link, C.D., 2008. Suppression of *in vivo* β -amyloid peptide toxicity by overexpression of the HSP-16.2 small chaperone protein. *J. Biol. Chem.* 283, 784–791. <https://doi.org/10.1074/jbc.M703339200>.
- Gao, Y., Tan, Lin, Yu, J.-T., Tan, Lan, 2018. Tau in Alzheimer's disease: mechanisms and therapeutic strategies. *CAR* 15, 283–300. <https://doi.org/10.2174/1567205014666170417111859>.
- Giacometti, J., Grubić-Kezele, T., 2020. Olive leaf polyphenols attenuate the clinical course of experimental autoimmune encephalomyelitis and provide neuroprotection by reducing oxidative stress, regulating microglia and SIRT1, and preserving myelin integrity. *Oxid. Med. Cell. Longev.* 6125638. <https://doi.org/10.1155/2020/6125638>, 2020.
- Godos, J., Currenti, W., Angelino, D., Mena, P., Castellano, S., Caraci, F., Galvano, F., Del Rio, D., Ferri, R., Grosso, G., 2020. Diet and mental health: review of the recent updates on molecular mechanisms. *Antioxidants* 9, 346. <https://doi.org/10.3390/antiox9040346>.

- Jin, C.H., So, Y.K., Han, S.N., Kim, J.-B., 2016. Isoeogomaketone upregulates heme oxygenase-1 in RAW264.7 cells via ROS/p38 MAPK/Nrf2 pathway. *Biomol. Therap.* 24, 510–516. <https://doi.org/10.4062/biomolther.2015.194>.
- Kumaran, A., Karunakaran, R.J., 2007. Activity-guided isolation and identification of free radical-scavenging components from an aqueous extract of *Coleus aromaticus*. *Food Chem.* 100, 356–361. <https://doi.org/10.1016/j.foodchem.2005.09.051>.
- Leri, M., Natalello, A., Bruzzzone, E., Stefani, M., Bucciantini, M., 2019. Oleuropein aglycone and hydroxytyrosol interfere differently with toxic A β 1-42 aggregation. *Food Chem. Toxicol.* 129, 1–12. <https://doi.org/10.1016/j.fct.2019.04.015>.
- Lockyer, S., Rowland, I., Spencer, J.P.E., Yaqoob, P., Stonehouse, W., 2017. Impact of phenolic-rich olive leaf extract on blood pressure, plasma lipids and inflammatory markers: a randomised controlled trial. *Eur. J. Nutr.* 56, 1421–1432. <https://doi.org/10.1007/s00394-016-1188-y>.
- Luccarini, I., Ed Dami, T., Grossi, C., Rigacci, S., Stefani, M., Casamenti, F., 2014. Oleuropein aglycone counteracts A β 42 toxicity in the rat brain. *Neurosci. Lett.* 558, 67–72. <https://doi.org/10.1016/j.neulet.2013.10.062>.
- Luo, S., Jiang, X., Jia, L., Tan, C., Li, M., Yang, Q., Du, Y., Ding, C., 2019. In vivo and in vitro antioxidant activities of methanol extracts from olive leaves on *Caenorhabditis elegans*. *Molecules* 24, 704. <https://doi.org/10.3390/molecules24040704>.
- Manzanares, P., Ruiz, E., Ballesteros, M., Negro, M.J., Gallego, F.J., López-Linares, J.C., Castro, E., 2017. Residual biomass potential in olive tree cultivation and olive oil industry in Spain: valorization proposal in a biorefinery context. *Spanish J. Agric. Res.* 15. <https://doi.org/10.5424/sjar/2017153-10868> e0206–e0206.
- Melov, S., Adlard, P.A., Morten, K., Johnson, F., Golden, T.R., Hinerfeld, D., Schilling, B., Mavros, C., Masters, C.L., Volitakis, I., Li, Q.-X., Laughton, K., Hubbard, A., Cherny, R.A., Gibson, B., Bush, A.L., 2007. Mitochondrial oxidative stress causes hyperphosphorylation of tau. *PLoS One* 2, e536. <https://doi.org/10.1371/journal.pone.0000536>.
- Mijatovic, S.A., Timotijevic, G.S., Miljkovic, D.M., Radovic, J.M., Maksimovic-Ivanic, D. D., Dekanski, D.P., Stosic-Grujicic, S.D., 2011. Multiple antimelanoma potential of dry olive leaf extract. *Int. J. Cancer* 128, 1955–1965. <https://doi.org/10.1002/ijc.25526>.
- Navarro-Hortal, M.D., Romero-Márquez, J.M., Esteban-Muñoz, A., Sánchez-González, C., Rivas-García, L., Llopis, J., Cianciosi, D., Giampieri, F., Sumalla-Cano, S., Battino, M., Quiles, J.L., 2021. Strawberry (*Fragaria* × *ananassa* cv. Romina) methanolic extract attenuates Alzheimer's beta amyloid production and oxidative stress by SKN-1/NRF and DAF-16/FOXO mediated mechanisms in *C. elegans*. *Food Chem.* 372, 131272. <https://doi.org/10.1016/j.foodchem.2021.131272>.
- Nicoli, F., Negro, C., Vergine, M., Aprile, A., Nutricati, E., Sabella, E., Miceli, A., Luvisi, A., De Bellis, L., 2019. Evaluation of phytochemical and antioxidant properties of 15 Italian *Olea europaea* L. Cultivar leaves. *Molecules* 24, 1998. <https://doi.org/10.3390/molecules24101998>.
- Oliveras-López, M.-J., Molina, J.J.M., Mir, M.V., Rey, E.F., Martín, F., de la Serrana, H.L.-G., 2013. Extra virgin olive oil (EVOO) consumption and antioxidant status in healthy institutionalized elderly humans. *Arch. Gerontol. Geriatr.* 57, 234–242. <https://doi.org/10.1016/j.archger.2013.04.002>.
- Omar, S.H., Scott, C.J., Hamlin, A.S., Obied, H.K., 2018. Olive biophenols reduces alzheimer's pathology in SH-SY5Y cells and APPswe mice. *Int. J. Mol. Sci.* 20, E125. <https://doi.org/10.3390/ijms20010125>.
- Orak, H.H., Karamac, M., Amarowicz, R., Orak, A., Penkacik, K., 2019. Genotype-related differences in the phenolic compound profile and antioxidant activity of extracts from olive (*Olea europaea* L.) leaves. *Molecules* 24, 1130. <https://doi.org/10.3390/molecules24061130>.
- Perez-Herrera, A., Rangel-Zuñiga, O.A., Delgado-Lista, J., Marin, C., Perez-Martinez, P., Tasset, I., Tunez, I., Quintana-Navarro, G.M., Lopez-Segura, F., Luque de Castro, M. D., Lopez-Miranda, J., Camargo, A., Perez-Jimenez, F., 2013. The antioxidants in oils heated at frying temperature, whether natural or added, could protect against postprandial oxidative stress in obese people. *Food Chem.* 138, 2250–2259. <https://doi.org/10.1016/j.foodchem.2012.12.023>.
- Quiles, J.L., Sánchez-González, C., Vera-Ramírez, L., Giampieri, F., Navarro-Hortal, M.D., Xiao, J., Llopis, J., Battino, M., Varela-López, A., 2020. Reductive stress, bioactive compounds, redox-active metals, and dormant tumor cell biology to develop redox-based tools for the treatment of cancer. *Antioxidants Redox Signal.* 33, 860–881. <https://doi.org/10.1089/ars.2020.8051>.
- Ranieri, M., Di Mise, A., Difonzo, G., Centrone, M., Venneri, M., Pellegrino, T., Russo, A., Mastrodonato, M., Caponio, F., Valenti, G., Tamma, G., 2019. Green olive leaf extract (OLE) provides cytoprotection in renal cells exposed to low doses of cadmium. *PLoS One* 14, e0214159. <https://doi.org/10.1371/journal.pone.0214159>.
- Re, R., Pellegrini, N., Proteggente, A., Pannala, A., Yang, M., Rice-Evans, C., 1999. Antioxidant activity applying an improved ABTS radical cation decolorization assay. *Free Radic. Biol. Med.* 26, 1231–1237. [https://doi.org/10.1016/s0891-5849\(98\)00315-3](https://doi.org/10.1016/s0891-5849(98)00315-3).
- Rigacci, S., Guidotti, V., Bucciantini, M., Nichino, D., Relini, A., Berti, A., Stefani, M., 2011. A β (1-42) aggregates into non-toxic amyloid assemblies in the presence of the natural polyphenol oleuropein aglycon. *Curr. Alzheimer Res.* 8, 841–852. <https://doi.org/10.2174/156720511798192682>.
- Robles-Almazan, M., Pulido-Moran, M., Moreno-Fernandez, J., Ramirez-Tortosa, C., Rodriguez-Garcia, C., Quiles, J.L., Ramirez-Tortosa, M., 2017. Hydroxytyrosol: bioavailability, toxicity, and clinical applications. *Food Res. Int.* 105, 654–667. <https://doi.org/10.1016/j.foodres.2017.11.053>.
- Romani, A., Ieri, F., Urciuoli, S., Noce, A., Marrone, G., Nediani, C., Bernini, R., 2019. Health effects of phenolic compounds found in extra-virgin olive oil, by-products, and leaf of *Olea europaea* L. *Nutrients* 11, E1776. <https://doi.org/10.3390/n11081776>.
- Sarbishegi, M., Charkhat Gorgich, E.A., Khajavi, O., Komeili, G., Salimi, S., 2018. The neuroprotective effects of hydro-alcoholic extract of olive (*Olea europaea* L.) leaf on rotenone-induced Parkinson's disease in rat. *Metab. Brain Dis.* 33, 79–88. <https://doi.org/10.1007/s11011-017-0131-0>.
- Singleton, V.L., Orthofer, R., Lamuela-Raventós, R.M., 1999. [14] Analysis of total phenols and other oxidation substrates and antioxidants by means of folin-ciocalteu reagent. In: *Methods in Enzymology, Oxidants and Antioxidants Part A*. Academic Press, pp. 152–178. [https://doi.org/10.1016/S0076-6879\(99\)99017-1](https://doi.org/10.1016/S0076-6879(99)99017-1).
- Tullet, J.M.A., Green, J.W., Au, C., Benedetto, A., Thompson, M.A., Clark, E., Gilliat, A.F., Young, A., Schmeisser, K., Gems, D., 2017. The SKN-1/Nrf2 transcription factor can protect against oxidative stress and increase lifespan in *C. elegans* by distinct mechanisms. *Aging Cell* 16, 1191–1194. <https://doi.org/10.1111/acel.12627>.
- Vogel, P., Kasper Machado, I., Garavaglia, J., Zani, V.T., de Souza, D., Morel Dal Bosco, S., 2014. Polyphenols benefits of olive leaf (*Olea europaea* L.) to human health. *Nutr. Hosp.* 31, 1427–1433. <https://doi.org/10.3305/nh.2015.31.3.8400>.
- World Health Organization, 2021a. Alzheimer's Disease Fact Sheet [WWW Document]. National Institute on Aging. URL, 12.21.21. <http://www.nia.nih.gov/health/alzheimers-disease-fact-sheet>.
- World Health Organization, 2021b. Dementia [WWW Document]. URL, 12.21.21. <https://www.who.int/news-room/fact-sheets/detail/dementia>.
- World Health Organization, 2020. The Top 10 Causes of Death [WWW Document]. URL, 12.21.21. <https://www.who.int/news-room/fact-sheets/detail/the-top-10-causes-of-death>.
- Wu, L.-X., Xu, Y.-Y., Yang, Z.-J., Feng, Q., 2018. Hydroxytyrosol and olive leaf extract exert cardioprotective effects by inhibiting GRP78 and CHOP expression. *J. Biomed. Res.* 32, 371–379. <https://doi.org/10.7555/JBR.32.20170111>.
- Zairi, A., Nour, S., Zarrouk, A., Haddad, H., khélifa, A., Achour, L., 2020. Phytochemical profile, cytotoxic, antioxidant, and allelopathic potentials of aqueous leaf extracts of *Olea europaea*. *Food Sci. Nutr.* 8, 4805–4813. <https://doi.org/10.1002/fsn3.1755>.
- Zecic, A., Braeckman, B.P., 2020. DAF-16/FoxO in *Caenorhabditis elegans* and its role in metabolic remodeling. *Cells* 9, 109. <https://doi.org/10.3390/cells9010109>.
- Zemva, J., Schubert, M., 2014. The role of neuronal insulin/insulin-like growth factor-1 signaling for the pathogenesis of Alzheimer's disease: possible therapeutic implications. *CNS Neurol. Disord. - Drug Targets* 13, 322–337. <https://doi.org/10.2174/18715273113126660141>.
- Zhi, D., Wang, D., Yang, W., Duan, Z., Zhu, S., Dong, J., Wang, Na, Wang, Ningbo, Fei, D., Zhang, Z., Wang, X., Wang, M., Li, H., 2017. Dianxianning improved amyloid β -induced pathological characteristics partially through DAF-2/DAF-16 insulin like pathway in transgenic *C. elegans*. *Sci. Rep.* 7, 11408. <https://doi.org/10.1038/s41598-017-11628-9>.